International Congress on Environmental Modelling and Software

7th International Congress on Environmental Modelling and Software - San Diego, California, USA - June 2014

Jun 17th, 3:40 PM - 5:20 PM

3D Model Construction of Water Supply System Pipes Based on GPR Images

David Ayala-Cabrera
Universitat Politècnica de València, daaycab@upv.es

Joaquín Izquierdo
Universitat Politècnica de València, jizquier@upv.es

Silvia J. Ocaña-Levario
Universitat Politècnica de València, silocle@upv.es

Rafael Pérez-García
Universitat Politècnica de València, rperez@upv.es

Ayala-Cabrera, David; Izquierdo, Joaquín; Ocaña-Levario, Silvia J.; and Pérez-García, Rafael, "3D Model Construction of Water Supply System Pipes Based on GPR Images" (2014). *International Congress on Environmental Modelling and Software*. 2.
https://scholarsarchive.byu.edu/iemssconference/2014/Stream-D/2

International Environmental Modelling and Software Society (iEMSs)
7th Intl. Congress on Env. Modelling and Software, San Diego, CA, USA,
Daniel P. Ames, Nigel W.T. Quinn, Andrea E. Rizzoli (Eds.)
http://www.iemss.org/society/index.php/iemss-2014-proceedings

3D Model Construction of Water Supply System Pipes Based on GPR Images

David Ayala-Cabrera [a], **Joaquín Izquierdo**[a], **Silvia J. Ocaña-Levario**[a], **and Rafael Pérez-García**[a]

[a] *FluIng-IMM, Universitat Poliècnica de València, Camino de Vera s/n edif. 5C, 46022, Valencia, Spain*
(daaycab, jizquier, silocle, rperez)@upv.es

Abstract: In this work, a GPR (ground penetrating radar) development is presented as a non-destructive technique. It allows the visualization of water supply system (WSS) pipelines buried into the ground. The main scope is in image (radargram) processing obtained from GPR, to obtain improved data visualization. For the application of the technique, laboratory essays have been conducted. These essays were performed by burying a commonly used pipe in a tank that emulates a small ground parcel. The images obtained were analysed and particular differences between them were observed. From this ensemble of images, a 3D model was generated to obtain better visualization and analysis of the pipeline. As a result, a clearer vision of the pipeline, as well as of other surrounding characteristics, was observed. This work is intended to obtain 3D models for an upgraded visualization of radargrams mainly focused on users that have poor knowledge of GPR and radargrams analysis. In the future, the development of a more powerful tool that allows the inspection of WSSs is pursued, allowing not only the location of pipelines, but also obtaining their depth, diameter and possible anomalies, among other interesting characteristics.

Keywords: pipe 3D models; image analysis and processing; water supply systems; non-destructive prospection methods; ground penetrating radar.

1 INTRODUCTION

Suitable knowledge of the layouts and characteristics (condition, age, e.g.) of water supply system (WSS) components (pipes, valves, etc.) is essential for efficiently and dynamically manage these systems. This knowledge is crucial to achieve such goals of WSS management as: illegal connection identification, water leakage detection and control, simulation and operation of networks, study of the evolution of pollutants into the networks, planning of supply systems, and maintenance, rehabilitation and renewal of components, among others. Non-invasive inspection methods for the detection of components in WSS have recently gained great significance in this regard. GPR is here selected due to its characteristics as a non-destructive method, which allows to discover layouts and features in both metallic and non-metallic pipes. GPR has also important applications in discovering other WSS characteristics such as water leaks in WSSs, Ayala-Cabrera et al. (2013).

The evaluation of GPR tests to analyze 3D objects is a common activity in various fields. For example, Dyana et al. (2012) considers the detection of landmines. Stratigraphic visualization in archeological excavation is considered in Pena et al. (2013). Civil engineering also provides some examples, such as the calibration of measurements on bridges, Heikkilä et al. (2010). There are many other examples of uses of GPR. Typically, volumes are built, on which profiles are made, either in depth or through surface layers. Subsequently, interpretations of those volumes are performed thus rendering the sought reconstruction. However, this process is complex and, to the difficulty of interpretation, adds the computational cost of managing the large amount of data (even with a single volume) that can be obtained with GPR surveys. In this paper, we propose to perform interpretations directly from the captured profiles and, subsequently, use them to generate 3D models. This seeks to simplify the process of constructing interpretations of GPR, thus reducing the change in dimensions and determining the model only as a step from 2D to 3D.

All in all, the main contribution of this work is to evaluate the feasibility of generating 3D models from images of GPR. The aim is to show the importance of advancing research toward the automatic interpretation of GPR images. Thus, understanding of the characteristics of the soil tested by using non-destructive testing by not highly qualified personnel is enhanced.

2 OVERALL APPROACH

Within the general purpose of this paper, proposing the use of GPR images (input) for the construction of 3D (output) models of buried objects, the approach particularly focuses on WSS pipes. The main difficulties of this process and the benefits to be gained once generated a 3D model include:

Difficulties

- The absence of a clear and precise protocol for performing GPR interpretations.
- The difficulty of displaying some items in the images of GPR; for example, in Ocaña-Levario (2014) it is established the difficulty of visualizing pipe materials, such as polyethylene (PE), polyvinyl chloride (PVC), asbestos cement (AC), cast iron (CI), in GPR images, with difficulty ordered by: PE $>$ PVC $>$ CA $>$ CI.
- Excessive noise in the images.
- Deformation of target objects due to the equipment characteristics and the electromagnetic characteristics of the environment, among others.
- Others.

Benefits

- Clear and understandable visualization of WSS components by the use of the GPR as a nondestructive method.
- Fostering the use of technologies such as augmented reality.
- Enabling hydraulic behavior study by using non-destructive techniques.
- Helping management activities of the WSS, such as maintenance, rehabilitation and general decision-making.

On this basis, this paper includes three processes to be performed: a) GPR image capture, b) development of contours for 3D models, and c) generation of a suitable mesh and of the 3D model. These processes are described in more detail below.

3 CAPTURE OF GPR IMAGES - CONFIGURATION OF TEST

The work in this paper presents the development of a laboratory case. In this section, the configuration of the tests performed is presented, whereby images from GPR were obtained. It should be noted that this document will call profiles to these images, since they are cross sections of the ground inspected.

In the acquisition of GPR profiles a plastic pipe was used. The selection of this material was made due to the complexity of identifying plastic objects in GPR images. Furthermore, the plastic materials are widely installed in WSS networks (especially, in secondary networks). The characteristics of the buried pipe are: a) material = PVC, b) outer diameter $d = 110$mm, c) length of the pipe $L = 500$mm. The selected pipe was buried in a tank with dimensions of 1.00 $\times$ 1.00 $\times$ 0.60m of useful volume, and the soil and material contained therein presents clay-loam features, as the material used to bury pipes in WSS. Once buried the pipe (in the case of pipe testing), the tank was covered with a polypropylene plate. A mesh was drawn on the cover plate, each line corresponding to one path for each of the profiles captured. A total of 22 profiles, 11 transversely and 11 longitudinally to the buried pipe, were taken. The characteristics of the tests are presented in Figure 1.

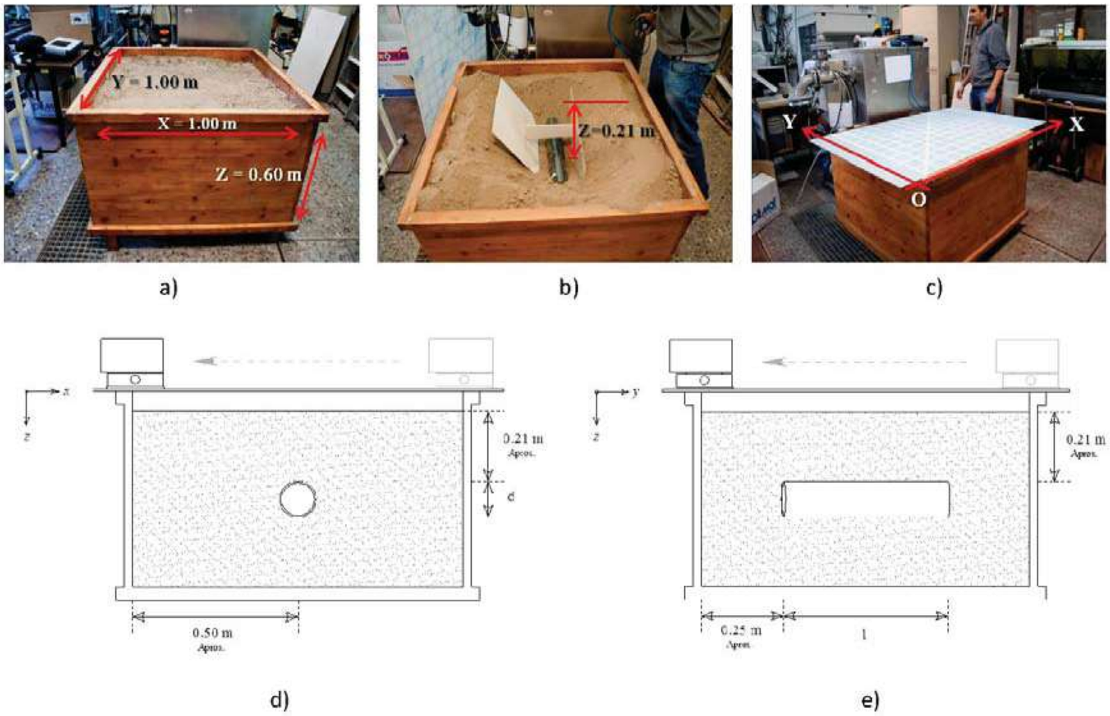

Figure 1. Configuration of the tests: (a) tank on which the tests are performed; (b) PVC pipe being buried, (c) the tank cover plate and mesh, (d-e) transversal and longitudinal sections of the tank, respectively.

4 CONTOURS FOR THE 3D MODEL

This section presents the proposed process to extract the contours for the GPR images. This process consists of the following steps: a) contrast, b) identification of ranges where the objects of interest are placed, c) demarcation of boundaries. This process is described below.

We have to keep in mind that one of the disadvantages in constructing 3D models from images of GPR is the absence of clear and repeatable protocols for making interpretations of these images. In this document, a contrast with a reference image for each GPR profile obtained is considered. This is done in order for the objects of interest to be clearly visible. The main input of this work is the raw data obtained from the GPR, visualized as radargrams. The received signals are stored in a matrix MR (raw radargram matrix), which is composed of m-vectors b_k, $k = 1, \ldots, n$ (traces), which represents the change in depth of the electromagnetic properties of the ground. We will represent this matrix by columns $MR = [b_1, b_2, \ldots, b_{n-1}, b_n]$. The length, m, of vector b_k, corresponds to the volume of data recorded in each track, which depends on the characteristics of the signal of the equipment used. The sample size is a parameter of the equipment, generally corresponding to sets of 512, 1024 and 2048 samples/trace for commercial equipment. In this study, 512 samples/trace, for a total of 20 ns/trace, were taken. From the set of measurements, s MR matrices, an average column vector of size m, $bc = \left(\sum_1^s \sum_1^k b_k\right) / (k \cdot s)$, may be calculated for the total set of traces obtained. Accumulating this vector consecutively n times, the reference matrix (white matrix), MW is built. The contrast matrix for each profile is given by $[MC_s] = abs\left([MR_s] - [MW]\right)$. The images obtained with these matrices are analyzed in detail, in order to find ways to provide information of the buried pipe and its boundary conditions.

To build the 3D model proposed in this paper, we focus on two objects of interest within the images. These two objects are the buried pipe and the inside of the tank. After several iterations, the best display for the pipe was found in a range of $[0\ 150]$ for cross sections, and $[0\ 100]$ for longitudinal profiles. The inner surface contour of the tank was observed in a range of $[0\ 100]$, both in cross and longitudinal profiles. On each of these images contours of the sought objects are manually delineated. Although this process is carried out manually in this work, the goal is to carry it out automatically. This manual process may serve in future research to corroborate the results obtained by automatic extraction techniques. An example of the applied process is shown in Figure 2. The aim is to improve the visualization in subsequent extraction of contours.

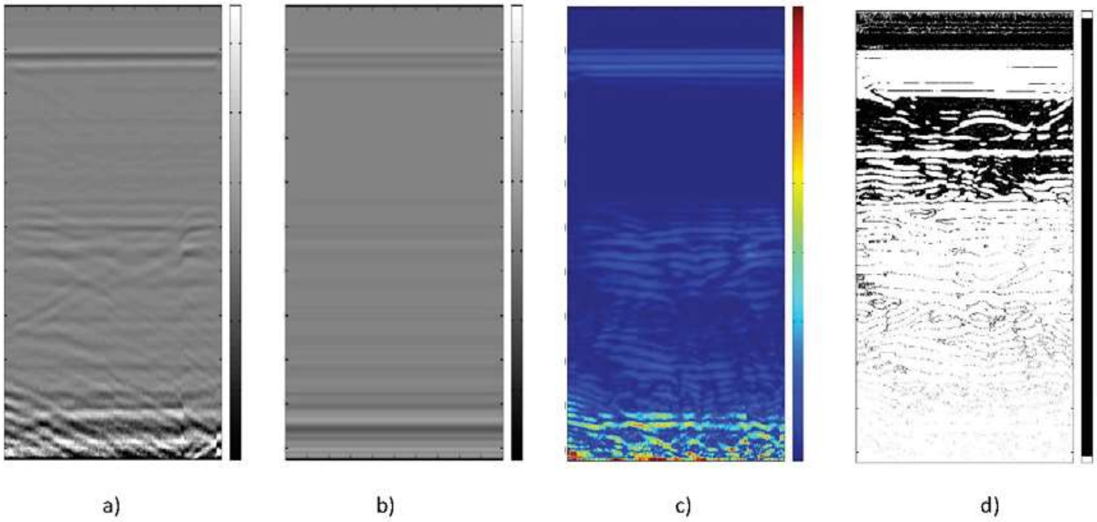

Figure 2. (a) Raw profile, MR matrix, (b) white matrix, MW, (c) contrast matrix, MC, and (d) selection of color range for the contrast matrix.

5 GENERATION OF THE MESH SYSTEM AND THE 3D MODEL

After having evaluated all the GPR captured profiles and extracted their contours, they are positioned spatially. The two objects of interest sought were treated separately, each one generating a different meshed network. The meshes generated in this study were constructed by the well-known Delaunay triangulation, which has become a de facto standard for the construction of various domain meshes, (Dey et al., 2012; Liu et al., 2010). This is the reason why we use it as a suitable tool to relate the obtained contours. This is justified because the main contribution of this work is to evaluate the feasibility of constructing 3D models from images of GPR.

The process of creating the mesh for the inner contour of the tank is shown in Figure 3.

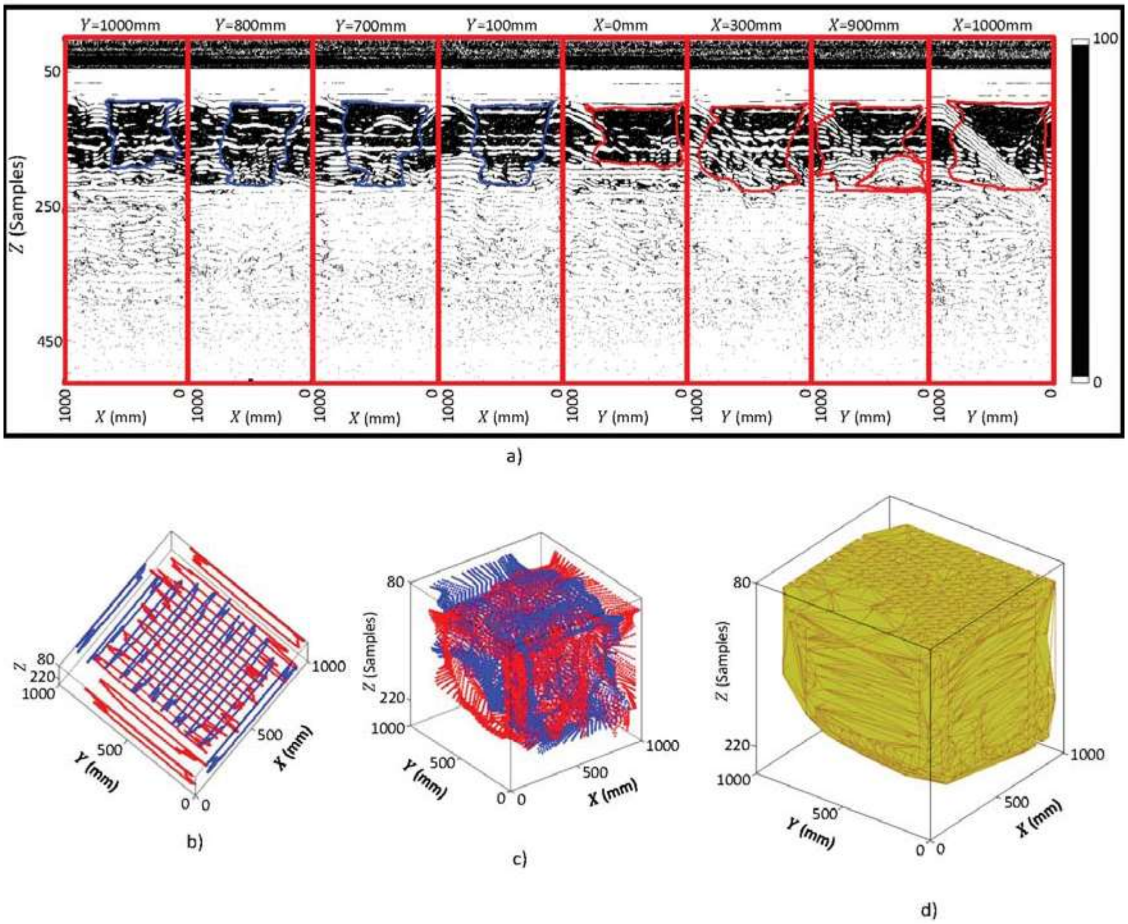

Figure 3. 3D reconstruction of the inner contour of the tank: (a) examples of manual extraction of the tank contours from GPR images, (b) spatial position of the transverse contours (blue lines) and longitudinal contours (red lines), (c) cloud of points, and d) mesh contour inside the tank.

In Figure 3a), some of the most relevant profiles obtained using GPR are presented. These profiles are shown with the implementation of the process to improve the visualization (contrast and range selection) and with defined contours. From the profiles it can be seen that the contour of the tank and what is contained in it represents less than 60% of the captured information. These internal contours of the tank are placed spatially, Figure 3b). In this work, two alignments of the contours are presented, which are the result of the transverse and the longitudinal profiles. Although the points may be subjected directly to the process of triangulation, to standardize herein the meshing, we decided to perform an interpolation of each alignment. From this interpolation alignments, a cloud of points was obtained, which is presented in Figure 3c). Through the triangulation the shape of the inner contour of the tank, Figure 3d), is obtained.

Profiles containing the buried pipe and its spatial location are presented in Figure 4.

The forms obtained in Figure 4, both for the cross sections of the pipe (a-f) and for the longitudinal profiles (g-i), present high correlation with each other, Figure 4j). It may be noted that with the measurements performed with GPR only the cross sections of the pipe can be observed. These cross sections provide indeed more information. This is the reason why, in the triangulation of the grid for 3D reconstruction of the pipe, only the contours obtained from the cross sections (a-f) were used. Longitudinal profiles (g-h) have been considered with the aim of verifying the results.

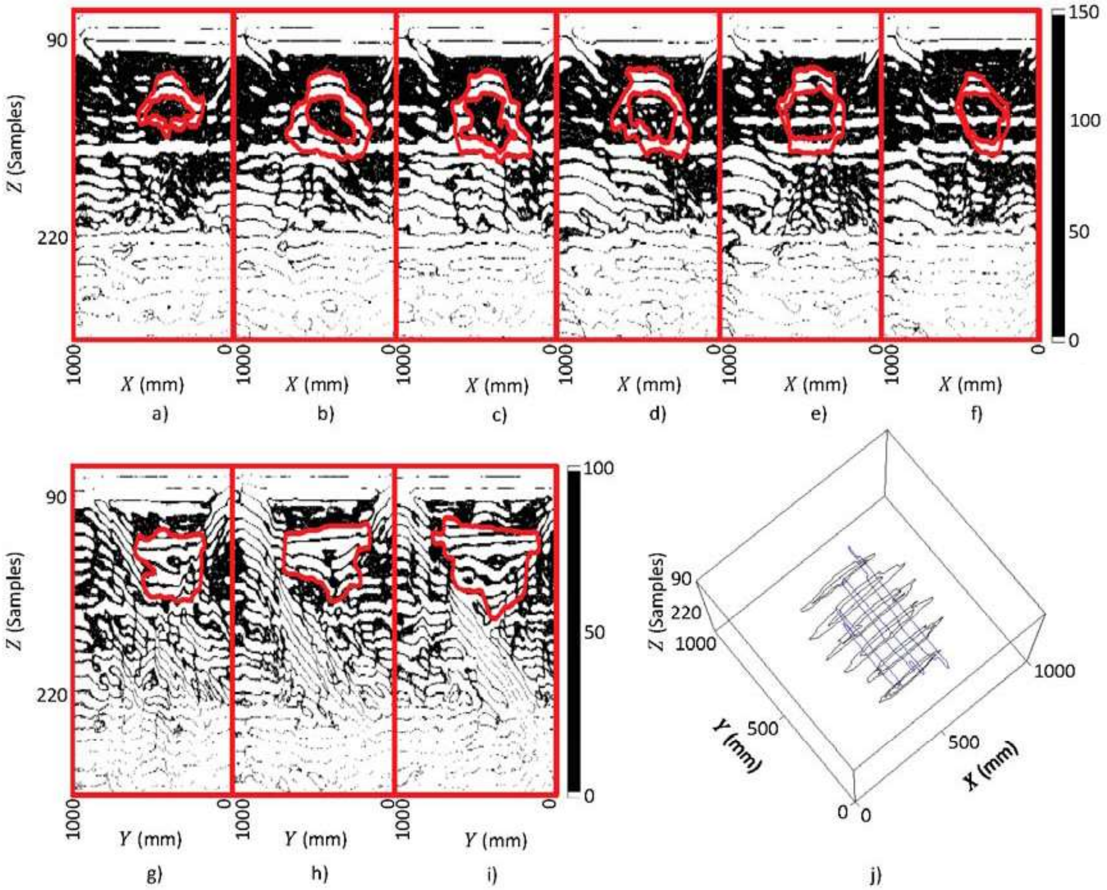

Figure 4. Manual extraction of contours of the buried pipe: (a-f) profiles cutting the pipe transversely, (g-i) profiles cutting the pipe longitudinally. (a) Y = 700mm, (b) Y = 600mm, (c) Y = 500mm, (d) Y = 400mm, (e) Y = 300mm, (f) Y = 200mm, (g) X = 400mm, (h) X = 500mm, (i) X = 600mm, and (j) spatial position of the transverse contours (black lines) and longitudinal contours (blue lines).

3D assembly of the two objects of interest, obtained in this document, from the GPR images is presented in Figure 5.

In Figure 5, we can see how it is possible to reconstruct a 3D model from the images obtained by the GPR. One can see that, in addition to the installed pipe, also the boundary conditions surrounding the pipe can be reconstructed. It can also be noted that the GPR interpretations, although not corresponding exactly to the installed dimensions, do provide an idea of the buried pipelines and their state. We claim, therefore, that it is possible to visually reconstruct pipelines made out of materials of such complex identification as plastic.

The deformations of both the pipe and the inner contour of the tank are explained by the signal path for each material. This can thus urges furthering the study of how signal-ground interactions occur, so that it is possible to resize and classify the pipes and their environment. However, the 3D model itself already gives us an idea of the buried objects. And, very importantly, this is accomplished by a

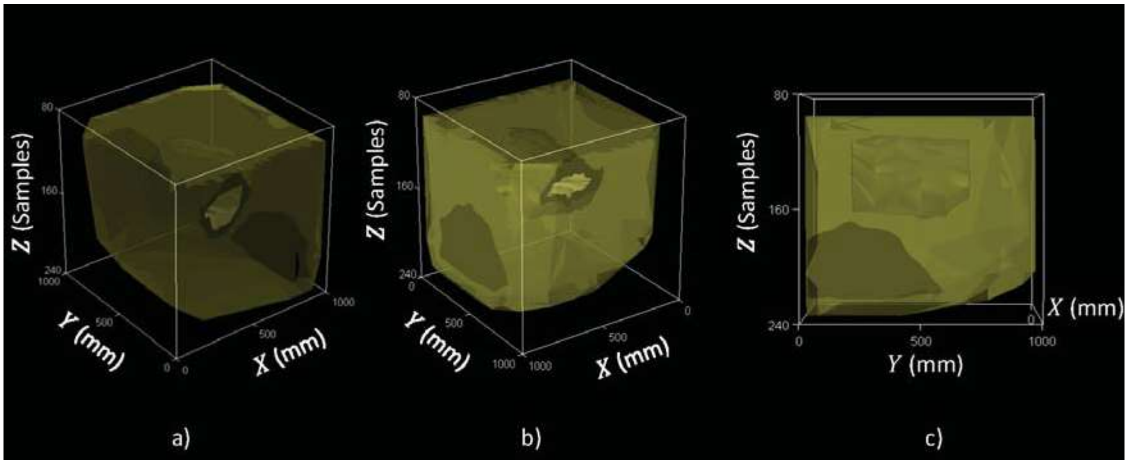

Figure 5. 3D model: (a-c) various points of view

non-destructive method such as the GPR.

6 CONCLUSIONS

The work performed has shown the feasibility of generating 3D models that are easily interpreted by not highly qualified personnel using GPR. Cases as complex as those posed by plastics pipes have been emphasized. Although interpretations have been performed manually, they show that there are more ways - beyond the classical identification of the first hyperbola - that can be used when studying GPR images. As a conclusion, we can state that these forms enable to obtain more understandable scenarios.

7 ACKNOWLEDGMENTS

Part of this work has been developed under the support of an FPI (Formación de Personal Investigador)-UPV (Universitat Politècnica de València) scholarship granted to the first author by the Programa de Ayudas de Investigación y Desarrollo (PAID) of the Universitat Politècnica de València.

REFERENCES

Ayala-Cabrera, D., Herrera, M., Izquierdo, J., Ocaña-Levario, S.J., Pérez-García, R., 2013. GPR-Based Water Leak Models in Water Distribution Systems. Sensors, 13, 15912-15936.
Dey, T.K., Janoos, F., Levine, J.A., 2012. Meshing interfaces of multi-label data with Delaunay refinement. Engineering with Computers, 28 (1), 71-82.
Dyana, A., Rao, C.H., Kuloor, R., 2012. 3D Segmentation of ground penetrating radar data for landmine detection. In Proceedings of the Ground Penetrating Radar (GPR), 2012 14th International Conference on, IEEE, pp. 858-863.
Heikkilä, R., Kivimäki, T., Leppälä, A., Mikkonen, M., Lasky, T.A., 2010. 3D calibration of GPR (ground penetrating radar) for bridge measurements - case Kajaani Varikko Bridge. In Proceedings of the 27th International Association for Automation and Robotics in Construction, ISARC, pp. 29-39
Liu, Y., Foteinos, P., Chernikov, A., Chrisochoides, N., 2010. Multi-tissue mesh generation for brain images. In Proceedings of the 19th International Meshing Roundtable, IMR, Chattanooga, TN, Springer-Verlag, Berlin, pp. 367-384.
Ocaña-Levario, S.J., 2014. Reconocimiento de patrones para la identificación de tuberías enterradas en sistemas de abastecimiento de agua a partir de imágenes de GPR. Master thesis, Universitat

Politècnica de València, Valencia, Spain.

Peña, J.A, Teixidó, T., 2013. Cover surfaces as a new technique for 3D GPR image enhancement. Archaeological applications. Repositorio Institucional de la Universidad de Granada. http://hdl.handle.net/10481/22949 (last accessed 20.03.14).